Mechanisms of Ligand Exchange Reactions, A Quantum Chemical Study of the Reaction $UO_2^{2+}(Aq) + HF(Aq) \rightarrow UO_2F^+(Aq) + H^+(Aq)$

Takashi Toraishi,[†,||] Timofei Privalov,*[,‡] Bernd Schimmelpfennig,[§] Ulf Wahlgren,[§] and Ingmar Grenthe*[,†]

Inorganic Chemistry, Department of Chemistry, The Royal Institute of Technology, Stockholm, Sweden, Organic Chemistry, Department of Chemistry, The Royal Institute of Technology, Stockholm, Sweden, AlbaNova University Center, Institute of Physics, Stockholm University, Stockholm, Sweden, and Department of Quantum Engineering and Systems Science, Graduate School of Engineering, The University of Tokyo, Tokyo, Japan

Received: April 17, 2003; In Final Form: August 26, 2003

The thermodynamics and the reaction mechanism for the reaction $UO_2^{2+}(aq) + HF(aq) \rightarrow UO_2F^+(aq) + H^+(aq)$ in water solution has been studied using quantum chemical methods. The solvent was modeled using the polarized medium method (CPCM) with additional water molecules in the second coordination sphere of the complexes studied. The overall reaction was divided into three steps that were analyzed separately. The quantum chemical study was made on the reaction step $[UO_2(H_2O)_5^{2+}],HF(H_2O)_n \rightarrow [UO_2F(H_2O)_4^+],H_3O^+(H_2O)_n$, with $n = 1$ and 2, where the species in the second coordination sphere are located outside the square brackets. The formation of the precursor complex and dissociation of the successor complex were described by the Fuoss equation. The geometry of the different precursor and successor complexes was in good agreement with known bond distances, and strong F- - -H- - -O, and/or O- - -H- - -O hydrogen bonds are an important structure element in all of them. The Gibbs energy, enthalpy, and entropy of reaction was calculated using the electronic energy at the MP2 level in the solvent, with thermal functions calculated at the SCF/B3LYP levels using the gas-phase geometry. The calculated Gibbs energy of reaction for $n = 2$ at 298.15 K was −35 kJ/mol at the HF and −25 kJ/mol at the B3LYP level after correction for a known systematic error in the HF bond energy; this compares favorably with the experimental value, −11 kJ/mol. The ligand exchange mechanism was explored by identification of a transition state where HF from the second sphere enters the first coordination sphere in an associative reaction. It was not possible to identify the same transition state from the successor side, indicating that the reaction mechanism consists of at least two steps. We suggest that the rate determining step is the entry of HF from the second to the first coordination sphere, with practically no bond-breaking as indicated by the small change in the H−F distance between precursor and transition state. This suggestion is supported by the experimentally observed reverse H/D isotope effect. The quantum chemical activation energy $\Delta U^{\neq}$ was 34 kJ/mol, close to the experimental activation enthalpy $\Delta H^{\neq} = 38$ kJ/mol.

Introduction

In some recent studies, we have investigated the rate and mechanism of water and fluoride exchange in different uranyl complexes using experimental[1−3] and quantum chemical[4,5] (ab initio) methods. The latter require a reasonably good model of the solvent in order to justify comparison with experimental data. For fluoride complexes of uranyl(VI),[6] we found it necessary to use specific water molecules in the second coordination sphere, in addition to the continuum solvent model (CPCM), to describe the main features of the experimental data. In the present study we will use quantum chemical methods to describe the thermodynamics and the reaction mechanism of the following more complex exchange reaction

$$UO_2^{2+}(aq) + HF(aq) \rightleftharpoons UO_2F^+(aq) + H^+(aq) \qquad (1)$$

for which the rate constant and the activation energy has been studied[7] in H_2O and 80% D_2O/H_2O at a constant perchloric acid concentration of 1.00 M, using dynamic NMR technique (^{17}O enriched UO_2^{2+}). The experimental rate equation, $v = k_{obs}[U^{17}O_2^{2+}][HF]$, is consistent with a mechanism that involves several steps, the formation of an outer-sphere complex between $UO_2^{2+}(aq)$ and HF, followed by proton transfer to water in the second coordination sphere and entry of fluoride/dissociation of water in the first coordination sphere. The experimental data do not provide information on the timing of the various bond formation/dissociation steps; however, the observed increase of the rate of exchange in D_2O as compared to H_2O is most likely an equilibrium isotope effect, indicating that hydrogen bond formation is important. The key issues in the present study are to investigate the thermodynamics and to obtain suggestions of

* To whom correspondence should be addressed. E-mail: priti@kth.se (T. P.); ingmarg@kth.se (I. G.).
[†] Inorganic Chemistry, The Royal Institute of Technology.
[‡] Organic Chemistry, The Royal Institute of Technology.
[§] AlbaNova University Center.
[||] The University of Tokyo.

10.1021/jp035033q CCC: $25.00
Published on Web 10/14/2003

the intimate mechanism for reaction 1 by using quantum chemical methods. This requires both proper theory methods and chemical models, where the level of detail of the solvent model is particularly important.

Methods

Computational Details. Energy consistent effective core potentials (ECP) of the Stuttgart type[8] were used in all calculations; previous studies[8−12] have proved their accuracy. We used the small core ECP with 32 electrons in the valence shell for uranium.[12] The oxygen and the fluorine atoms were described by the same type of energy consistent ECP's,[13] with polarizing d-functions included in the basis set; for hydrogen, we used basis set parameters suggested by Huzinaga[14] with 5s functions contracted to 3s. The geometry optimizations were made using this hydrogen basis set, while a diffuse *p*-function with the exponent 0.8 was added for the energy calculations at the correlated level. In the following sections, we refer to the first basis set as "small", while the latter one is described as "big".

The calculations were carried out using the program packages Molcas5[15] and Gaussian98,[16] with geometries optimized at the SCF/B3LYP level using gradient technique. The geometry of the precursor and successor complexes was initially optimized without symmetry constraints. Some of the refined structures turned out to have symmetry close to C_s; in these cases, we repeated the geometry optimization using this symmetry constraint; the energy difference between the constrained and unconstrained models was small, $\approx$ 3 kJ/mol, (see Supporting Information Table S2). The possibility to use symmetry constraints was an obvious advantage for the computationally expensive series of transition state geometry optimizations.

Correlation effects estimated at the MP2 and B3LYP levels were obtained by single-point calculations at the geometry optimized at the SCF and B3LYP levels, respectively. In the MP2 level calculations, the 5*s*, 5*p*, and 5*d* shells of uranium were kept frozen. Solvent effects were estimated within CPCM (polarized continuum model) as implemented in Molcas[17] and Gaussian98; for computational reasons, it was not possible to include a complete second coordination sphere in the models. The first step in the quantum chemical modeling was to study the complexes and reactions in gas-phase with a few explicitly treated water molecules (geometry optimization of the precursor/successor complexes without use of the continuum solvent model). This was followed by inclusion of a continuum solvent by using the CPCM model. Our previous experience[4−6] indicates that such an approach often is sufficient to describe experimental observations rather well.

In a previous communication,[19] we have shown that it is necessary to use extended basis sets to describe consistently the H−F and U−F bonds. Therefore, we investigated how the calculated reaction energies depend on the choice of basis sets; this was done using symmetry constrained precursor/successor models.

The SCF gas-phase geometry was the starting point for exploring the configuration space in order to find possible reaction pathways. The search for transition states was initiated starting from both the precursor complex $[UO_2(H_2O)_5^{2+}],HF(H_2O)_n$ and the successor complex $[UO_2(H_2O)_4F^+],H_3O^+(H_2O)_n$, by calculating the energy variation along the assumed reaction coordinate. As described later, most of the attempts failed, and it was only possible to identify a single transition state by following the U−F reaction coordinate in the system with $n = 2$. This was achieved by stepwise changes of the U−F distance and optimizing the geometry for each step at constant U−F distance; the calculations were very time-consuming due to the slow geometry convergence. When a single imaginary frequency was found, we tried to follow this to locate the transition state. However, the automated procedure failed, and we had to resort to the much more time-consuming mapping of the configuration space along the assumed reaction pathway. The Gibbs energy, enthalpy, and entropy of reaction were estimated from the MP2 and B3LYP energy within the CPCM model, the partition functions were obtained from the gas-phase frequencies calculated at the SCF and B3LYP levels using Gaussian98.

Model Reactions. The experimental equilibrium constant, log $K(1)$ and the Gibbs energy of reaction, $\Delta G°$, for the stoichiometric reaction 1 is equal to 1.91 ± 0.13[19] and -10.9 kJ/mol, respectively. To compare them with the values calculated by theory, we have divided reaction 1 into the following three reactions:

$$UO_2(H_2O)_5^{2+} + HF(H_2O)_n \rightarrow [UO_2(H_2O)_5^{2+}],HF(H_2O)_n \quad (2)$$

$$[UO_2(H_2O)_5^{2+}],HF(H_2O)_n \rightarrow [UO_2(H_2O)_4F^+],H_3O^+(H_2O)_n \quad (3)$$

$$[UO_2(H_2O)_4F^+],H_3O^+(H_2O)_n \rightarrow [UO_2(H_2O)_4F^+] + H_3O^+(H_2O)_n \quad (4)$$

where n denotes the number of water molecules in the chemical models tested; species in the second coordination sphere are outside the square brackets. The equilibrium constants for the outer-sphere reactions 2 and 4 estimated using the Fuoss equation in ref 1 a and b are 0.3 M^{-1} and 13.5 M, respectively, while that for the intra-molecular reaction 3 was obtained by quantum chemical methods. Reactions 2 and 4 are diffusion controlled, and reaction 3 must therefore contain the rate determining step. Our focus is on reaction 3 with the analysis of the energy and structure of the precursor and successor complexes, $[UO_2(H_2O)_5^{2+}],HF(H_2O)_n$ and $[UO_2(H_2O)_4F^+],H_3O^+(H_2O)_n$, and the transition state along the proposed reaction pathway. We have tested models with $n = 1$ and 2 and have, for comparison, also included structures and electronic energies of the complexes with $n = 0$.

Results

Structures of the Precursor and Successor Complexes in the $UO_2(H_2O)_5^{2+} - HF(H_2O)_n$ Models. The bond distances of the precursor/successor complexes with $n = 0-2$ are shown in Table 1. All bond distances are in good agreement with crystallographic and EXAFS data; the H_3O^+ unit has a trigonal planar geometry, as compared to flattened pyramid geometry in solid-state structures. Coordinates and absolute energies are given in Tables S1, S2, and S3. We identified two different precursor geometries for the model complex $[UO_2(H_2O)_5^{2+}],HF,(H_2O)$, one close to the C_s symmetry, Figure 1A, and the other one without symmetry, Figure 1B; the latter is less stable by 26.6 kJ/mol (gas phase, SCF). The geometry of the "symmetric" precursor was also obtained using C_s symmetry constraints; the geometry was very close to that without symmetry constraint (Figure 1D), and the total energy was 0.89 kJ/mol higher. A comparison between the structures in Figure 1, parts A and B shows the importance of hydrogen bonding, the F- - -H distance is strongly dependent on the interactions

TABLE 1: Calculated Bond Distances at the SCF Level in the Precursor/Successor Complexes with $n = 0, 1, 2$[a]

complex figure (symmetry)	U−F	H−F	$H_2O\cdots HF$	F···HOH (1)	F···HOH (2)	$U\cdots OH_2$ (trans water)	FUO_{yl} angle (degree)	$HOH-OH_2$ (2*nd* sphere−3*rd* sphere)
precursor figure 1A (C_1)	3.97	0.97	1.46	1.80	1.83	2.49	65.54	
precursor figure 1B (C_1)	4.02	0.92	1.74	2.86	1.74	2.50	58.46	
successor figure 1C (C_1)	2.25	1.49	0.99	2.44	3.35		92.45	
precursor figure 1D (C_s)	4.02	0.97	1.46	1.82	1.82	2.49	67.30	
successor figure 2 (Cs)	2.26	1.49	0.99	2.64	2.64		91.84	1.44
Precursor Figure 3A (C_1)	3.96	1.01	1.33	1.74	1.74	2.49	68.74	1.66
successor figure 3B (C_s)	2.25	1.45	1.00	3.182	3.181	4.28	90.78	1.47
figure 4A (C_s)	4.09	0.91		2.03	2.03	2.49	61.44	
figure 4B (C_s)	2.13			2.35	2.34	3.84	94.12	
TS Figure 5 (C_s)	2.60	1.03	1.31	2.30	2.30	2.48	70.54	1.64

[a] Bond distances are in Å.

with water in the second coordination sphere. In the symmetric precursor complexes (Figure 1A), the F−H distance is 0.97 Å, with H participating in strong linear hydrogen bonding (the H_2O- - -HF distance is 1.47 Å). In the asymmetric precursor (Figure 1B), the H_2O- - -HF distance is 0.92 Å, close to the value in gas-phase, a result of the much weaker, slightly bent, hydrogen bond to water (the distance H_2O- - -HF is 1.74 Å).

We found only one nonsymmetric successor complex; its geometry indicates that there are two equivalent structures (cf. Figure 1C). This was confirmed by a geometry optimization using C_s symmetry, where a frequency calculation showed that the symmetric successor has one and the nonsymmetric successor no imaginary frequency. The former corresponds to a translation movement between the two possible HF locations with the activation energy 3.2 kJ/mol. The geometry of the transition state is shown in Figure 2.

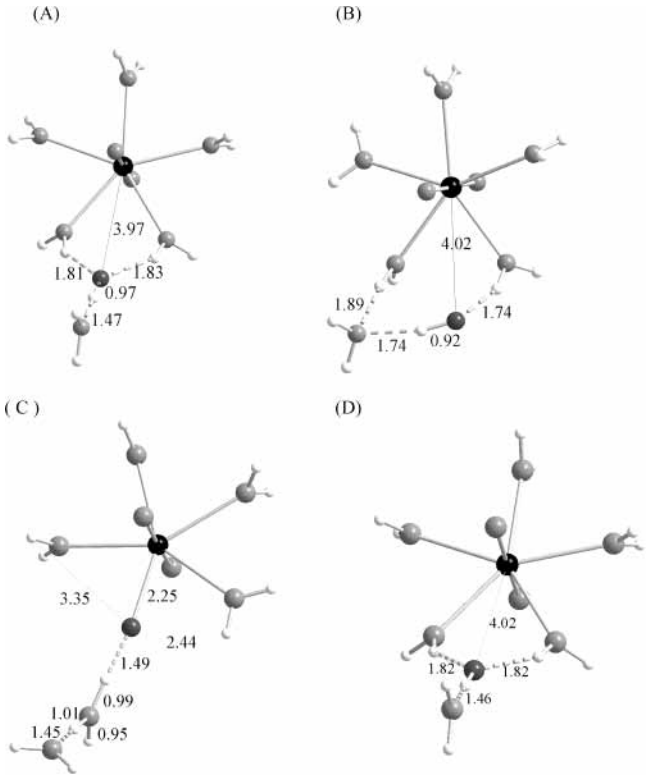

Figure 1. Precursor/successor complexes $[UO_2(H_2O)_5^{2+}]$,$HF(H_2O)$/$[UO_2(H_2O)_4F^+]$, $H_3O^+(H_2O)$ as optimized without symmetry constraints. (A) Precursor with geometry close to C_s. (B) Precursor complex with an asymmetric bonding of HF and water in the second coordination sphere. (C) The (nonsymmetric) successor complex. The dashed lines indicate hydrogen bond interactions. The bond distances are given in Å. There are two possible locations of the fluoride in C, the one shown here and the other where the distances $H_2O(1)$ and $H_2O(2)$ are 2.44 and 3.25 Å, respectively. (D) The symmetrical analogue of the precursor complex from (A) optimized with $n = 1$ (6 water molecules), within the C_s point group.

The structures of the precursor and successor complexes with $n = 2$, $[UO_2(H_2O)_5^{2+}]$,$HF(H_2O)_2]$ and $(H_2O)[(UO_2F(H_2O)_4^+],(H_3O^+)(H_2O)]$, are shown in Figure 3, parts A, B, respectively. Both have symmetry close to C_s, and the energy difference between structures optimized with and without symmetry constraints is negligible (see Table S2, the energy difference is less than 0.004kJ/mol). Strong, slightly asymmetric hydrogen bonds, $F-H\cdots(OH_2)_2$ and $F^-\cdots(H_3O^+)(H_2O)$, respectively, are important elements in both the precursor and successor structures. The F−H distance, 1.01 Å, is longer than the gas-phase value and also slightly longer than that found in the symmetric precursor with $n = 1$.

The symmetry plane through the UO_2 group and the fluoride suggests a reaction pathway that involves a proton transfer from the outer-sphere HF to the third sphere ($H_2O\cdots H_2O$) group, and with the release of the coordinated water in trans-position to the entering fluoride. However, as described in the following section, the mechanism is more complex.

All calculations for the model system with $n = 0$ were made using symmetry constraints; there is no stable successor complex $[UO_2(H_2O)_4F^+](H_3O^+)$. Optimization of the successor geometry (Figure 4B) results in proton transfer from H_3O^+ to F^-, and therefore only the structures of $[UO_2(H_2O)_5^{2+}]$,HF and $[UO_2(H_2O)_4F^+]$ are reported (cf. Figure 4).

The F−H distance in the precursor is 0.91 Å, close to the gas-phase value, while the U−F distance in the successor, 2.13 Å, is about 0.10 Å shorter than the value found for the successor complexes with $n = 1$ or 2, and that in $UO_2F_4^{2-}$ (ref 7).

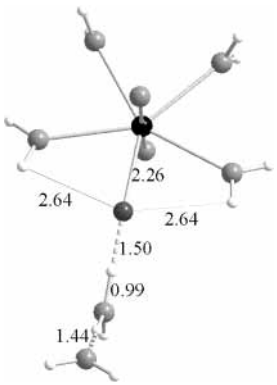

Figure 2. The successor complex $[UO_2(H_2O)_4F^+],H_3O^+(H_2O)$ optimized in C_s symmetry; this is not a stable structure but represents a transition state (cf. text). The dashed lines indicate hydrogen bond interactions. The bond distances are given in Å.

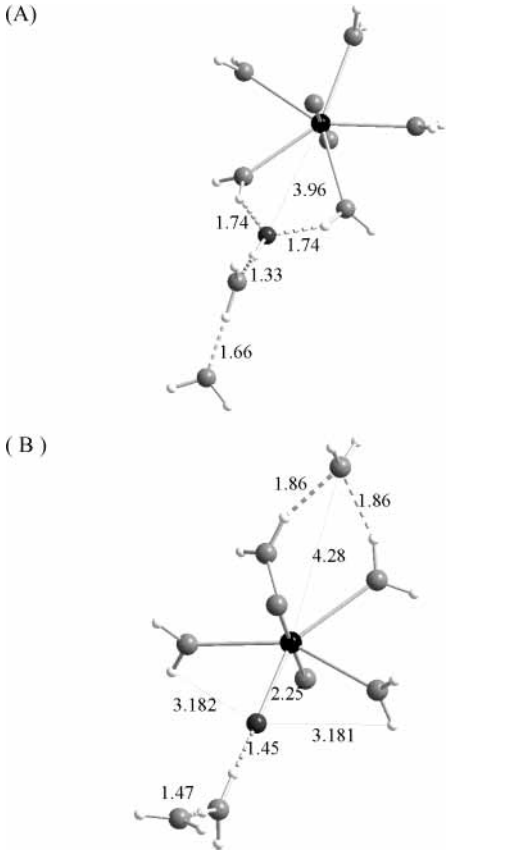

Figure 3. Precursor/successor complexes with seven water molecules optimized without symmetry constraints. Note the very small deviation of the geometry from C_s symmetry. (A) The structure of the precursor complex $[UO_2(H_2O)_5^{2+}],HF(H_2O)_2$. (B) The structure of the successor complex $[UO_2(H_2O)_4F^+],H_3O^+(H_2O)_2$. The hydrogen bonds are dashed, and all bond distances are given in Å.

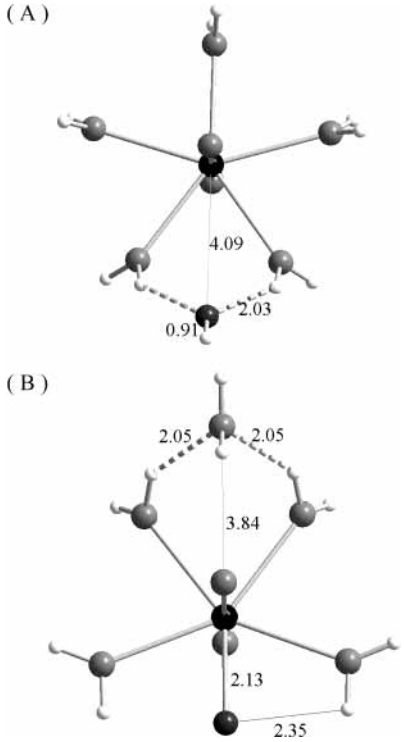

Figure 4. (A) The precursor complex $[UO_2(H_2O)_5^{2+}],HF$. (B) The inner coordination sphere of the successor complex $[UO_2(H_2O)_4F^+](H_2O)$. The hydrogen bonds are dashed, and all bond distances are given in Å.

The Thermodynamics of the Precursor/Successor Reaction. The SCF, MP2, and B3LYP electronic energy changes, ΔU, for the "precursor → successor" reaction 3 for $n = 1$ and 2 are given in Table 2 for the gas phase and solvent calculations with small and large basis sets. The entropy $S°$, zero point energy, and temperature functions for the enthalpy and Gibbs free energy, $H^{corr}(T)$ and $G^{corr}(T)$, obtained from the frequency calculations are given in Table S4. The change in enthalpy, $\Delta H°$ and Gibbs free energy, $\Delta G°$ for reaction 3 are given in Table 3; they were obtained using the MP2 and B3LYP level electronic energies. The B3LYP data were used to compare the electronic energy and the partition functions at the same level of theory. The small differences between the SCF and B3LYP frequencies indicate (Table S4) that the SCF level thermal functions are quite good for the calculations of the enthalpy and Gibbs free energy changes. For reaction 3, with $n = 1$ and the symmetric precursor and successor complexes, the change in the pure electronic energy at the MP2 level in the gas phase is −22.8 kJ/mol using the small and −13.9 kJ/mol using the large basis set. The difference is small, 9 kJ/mol, compared to that between the symmetric and nonsymmetric structure models, −29.8 kJ/mol. For reaction 3 with $n = 2$, the MP2 value of ΔU for the gas-phase reaction is −38.9 and −32.9 kJ/mol for the small and large basis sets, respectively, indicating good stability of the results with the change of basis set. The B3LYP value of ΔU obtained with the large basis set is −45.4 kJ/mol.

The corresponding energies of reaction in the solvent for the two models are given in Table 1. For the model with six water molecules, the effect of adding CPCM is 40 kJ/mol, while it is only 24 kJ/mol for the model with seven water molecules. However, the net energy change at the MP2 level with addition of CPCM is very similar for both models: −57 and −54 kJ/mol.

TABLE 2: The Electronic Energy Change, ΔU (in kJ/mol), at the HF, MP2, and B3LYP Levels for the Model Reactions with Six and Seven Water Molecules

medium	basis set	level of computation	symmetry constraint	ΔU (kJ/mol)
model with 6 water molecules				
gas	small	SCF	no (precursor from figure 1A)	−14.62
gas	small	SCF	C_s	−11.44
gas	small	MP2	C_s	−22.81
gas	large	MP2	C_s	−13.91
solvent (CPCM)	large	MP2	C_s	−54
gas	small	SCF	no (precursor from figure 1B)	−41.20
model with 7 water molecules				
gas	small	SCF	no	−33.32
gas	small	SCF	C_s	−33.32
gas	small	MP2	C_s	−38.92
gas	large	MP2	C_s	−32.90
gas	large	B3LYP	C_s	−45.40
solvent (CPCM)	small	MP2	C_s	−66.58
solvent (CPCM)	large	MP2/B3LYP	C_s	−56.90/−60.02

It seems appropriate to discuss in more detail the difference in the combined solvent and correlation effects for the two models. These differences cannot be explained by large changes in correlation contributions, as an estimate at the MP2 level gives small and very similar results for the six- and seven-water systems: the difference between the SCF (small basis) and MP2 (large basis) level electronic reaction energies is 3 and 0.32 kJ/mol, respectively. The increase of the basis set (addition of *p*-basis functions for H atoms) affects the MP2 energies in both models in a very similar fashion, an increase in ΔU with 9 and 6 kJ/mol, respectively, for the six- and seven-water models.

TABLE 3: The Electronic Energies, ΔU (kJ/mol) at the MP2 and B3LYP Levels with the Large Basis Set in the Gas Phase and Solvent (within the CPCM model); the Enthalpies of Reaction, $\Delta H°$ (kJ/mol); the Gibbs Free Energies of Reaction, $\Delta G°$ (kJ/mol); and the Molar Entropy, $S°$ (J/mol/K) for the Precursor and Successor Complexes[a]

reaction model	ΔU (kJ/mol) gas/solvent	$\Delta H°$ (kJ/mol) gas/solvent	$\Delta G°$ (kJ/mol) gas/solvent	S° (method) J/mol/K prec/succ
6 waters (C_s symmetry) MP2	−14/−54	−19/−56	−16/−56	(SCF) 642/633
7 waters (C_s symmetry) MP2	−33/−57	−31/−55	−27/−50	(SCF) 703/690
7 waters (C_s symmetry) B3LYP	−45/−60	−49/−56	−39/−58	(B3LYP) 698/705

[a] The reference temperature is 298.15 K.

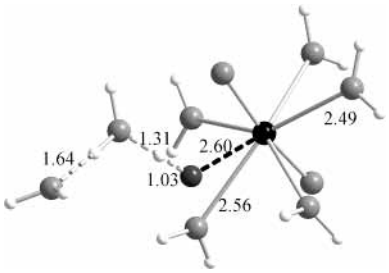

Figure 5. The suggested transition state for the transfer of HF from the second to the first coordination sphere in the reaction $[UO_2(H_2O)_5^{2+}],HF(H_2O)_2 \rightarrow [UO_2(H_2O)_4F^+],H_3O^+(H_2O)$. Uranium is six coordinated with a short distance, 2.60 Å between uranium and the entering HF, indicating an associative reaction mechanism. The distances F- - -H and H- - -OH_2 in the linear hydrogen bond are essentially the same as those in the precursor complex (Figure 2A). The black dashed line denotes the entering HF and the gray dashed lines hydrogen bonds.

Therefore, the difference in the reaction energy at MP2 level with addition of CPCM is generated solely by the difference in CPCM contributions to the energy of the precursor/successor complexes.

The successor complex in Figure 3B has one water molecule at the second coordination sphere, as compared to the successor complex in Figure 1C. It is reasonable to suggest that some of the solvent effects are already accounted for at the SCF level for the successor in Figure 3B, due to the presence of the water molecule in the second coordination sphere. This would most probably give rise to a more stable successor complex and larger reaction energy for the model with seven waters as compared to that with six waters. The CPCM is mainly used to mimic the bulk water solvent. In agreement with our previous experience,[4−6] the CPCM effect becomes smaller for the system with more water molecules, as expected (cf. Table. 1).

The DFT results agree well, within less than 13 kJ/mol, with the results obtained at the MP2 level. The enthalpy and Gibbs energies of reaction are obtained as described above, using the electronic energy from the large basis set calculations given in Table 3. By combining the quantum chemical Gibbs energy of reaction with the estimated outer-sphere equilibrium constants for reactions 2 and 4, we obtain an estimated Gibbs energy of reaction 1 (at the MP2 level) equal to −57 and −50kJ/mol for $n = 1$ and 2, respectively, and −58 kJ/mol for $n = 2$ with B3LYP. The corresponding experimental value is -10.9 ± 0.7 kJ/mol; the difference is significant. However, in a previous study,[19] we have used experimental thermodynamic data for gas-phase reactions in the U(VI)−H_2O−HF system to estimate the accuracy of our quantum chemical methods. This study indicates that there is a systematic error in reactions where HF participates and that it is possible to make an empirical correction of this error and thereby to obtain a good agreement between experiment and theory for a large number of reactions. The correction at the MP2 level is approximately −18 kJ/mol for each HF reactant and −33 kJ/mol at the B3LYP level (based on the results for reaction 2 in ref 17). Applying this correction to reaction 3, we obtain $\Delta G°$(eq 3) = −41 and −35 kJ/mol for $n = 1$ and 2 at the MP2 level, respectively, and −25 kJ/mol for $n = 2$ at the B3LYP level. The difference between the experimental and theory based thermodynamic data is now satisfactory at the B3LYP level, but is still fairly large at the MP2 level, although it seems to decrease with increasing number of water molecules in the model. The application of the HF correction from ref 13 is quite crude, and the large correction at the B3LYP level makes the estimated $\Delta G°$(eq 3) uncertain. However, it does provide a strong indication that the $\Delta G°$(eq 3) is underestimated by some 20−30 kJ/mol in the calculations.

Ab Initio Studies of the Reaction Pathway. The determination of the possible transition states (TS) and intermediates is the key to an appropriate description of the reaction pathway with ab initio methods. An obvious difficulty in the search for the transition state for reaction 3 is that it may not be an elementary reaction. In addition, the large number of degrees of freedom in the complexes makes it difficult to select an appropriate reaction coordinate. We will therefore give a rather detailed description of the attempts made to localize transition states. All attempts in the model with $n = 1$ failed. Our efforts were therefore concentrated on the reaction with $n = 2$ where we started from the precursor complex using the U−F distance as the reaction coordinate. The HF in the precursor is located outside the equatorial plane in $UO_2(H_2O)_5^{2+}$ at a distance of 3.96 Å from uranium; the geometry is similar to that found for the $UO_2(H_2O)_6^{2+}$ intermediate in the associative water exchange mechanism between $UO_2(H_2O)_5^{2+}$ and the water solvent.[4] The results of the transition state search are shown as black circles in Figure 6, where the energy of the geometry optimized complexes with C_s symmetry are plotted at different U−F distances. Starting from the precursor, it was possible to follow the U−F distance from 3.96 to 2.60 Å; at shorter distances, the calculations failed. We then tried to approach the transition state from the successor, starting from a U−F distance of 2.26 Å and increasing this stepwise; however, at a U−F distance of 2.35 Å, the calculations failed again. The fact that we could not identify the transition state starting from the successor complex shows that the reaction pathway cannot be described by using the U−F distance as the single reaction coordinate; reaction 3 is not an elementary reaction. A frequency analysis made at the U−F distances 2.35, 2.60, 2.65, 2.70, 2.75, and 2.85 Å showed a single imaginary frequency at 2.60, 2.65, 2.70 and 2.75 Å, consistent with a saddle point; the imaginary frequency corresponds to the movement of the [HF,$2H_2O$] group closer to the U atom. At the other distances, we found two or more imaginary frequencies, indicating that the structures are not located along the reaction pathway of lowest energy. The first part of the potential energy−reaction coordinate curve has a very broad maximum, and we have taken the geometry at the U−F distance of 2.60 Å (Figure 5) as representative for the transition state. In this structure, the five spectator water molecules have moved out of the equatorial plane, but with only a small increase in their distance to uranium. There is a

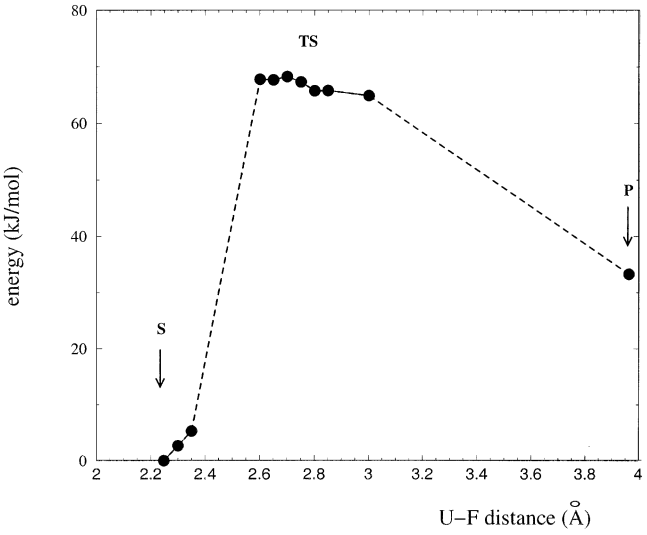

Figure 6. The electronic energy versus the reaction coordinate (the U−F distance) for the exchange of HF between the first and second coordination sphere in the complex $[UO_2(H_2O)_5^{2+}]$,$HF(H_2O)_2$; reaction 3. "S" and "P" mark successor and precursor, respectively. The energy is given in kJ/mol and the U−F distance in Å. The dark black circles denote the optimized geometries at the SCF level at the gas phase with the U−F distance constrained during the geometry optimization (see text).

significant change in the orientation of the water molecules on both sides of the entering HF between the precursor and the transition state. The increase in the F−H distance between the precursor and the assumed transition state is very small, 0.015 Å, with no change in the hydrogen bond donor−acceptor distance F- - -O, indicating that there is no bond breaking in HF. The F- - -H- - -O group is close to linear with a short F- - -O distance of 2.34 Å, indicating very strong hydrogen bonding. We suggest that the first step in the (composite) reaction 3 is the entry of HF into the first coordination sphere of uranium. From the geometry of the precursor and the transition state, it is obvious that this reaction step is associative, as found in a previous study[4] of ligand exchange in $UO_2(H_2O)_5^{2+}$ and $UO_2(oxalate)_2(H_2O)^{2-}$. The activation energy is estimated to 34 kJ/mol, based on the very small energy differences, a fraction of a kJ/mol, between the structures along the broad maximum in the pathway shown in Figure 6. The transfer of water from the first to the second coordination sphere must take place after the entry of HF in the first coordination sphere, but as indicated above, it was not possible to identify a transition state starting from the successor complex using the U − OH_2 distance as reaction coordinate. It seems probable that there are more complexes of similar energy with different location of the second-sphere water molecule, but our resources do not allow us to pursue all these possibilities or to use a model with a larger number of water molecules in the second coordination sphere, and we can therefore only obtain information on the first part of the reaction pathway.

Our results strongly suggest a reaction mechanism with at least two steps, where we only have information on the first one. A two-step reaction requires an intermediate that we have been unable to locate. This is not surprising, as reactive intermediates have low activation barriers and are therefore difficult to identify; some examples are given in one of our previous studies.[21] The second step in the reaction mechanism must involve transfer of water from the first to the second coordination sphere, and we may speculate on the activation energy. In a previous study,[5] we have estimated the activation energy, $\Delta U^{\neq} = 19$ kJ/mol, for the water exchange along the *A/I* pathway in the reactions $[UO_2(H_2O)_5]^{2+}$,(H_2O); this may be a good estimate also for the activation energy for the release of water from $[UO_2(H_2O)_5HF(H_2O)_2^{2+}]^{\neq}$, or a corresponding intermediate. The activation energy for the entry of HF in the first coordination sphere is higher, 34 kJ/mol, in fair agreement with the experimental value $\Delta H^{\neq} = 38$ kJ/mol and may therefore refer to the rate-determining step in the exchange reaction

$$UO_2^{2+}(aq) + HF(aq) \rightleftharpoons UO_2F^{+}(aq) + H^{+}(aq)$$

Conclusion

Comparison with Experimental Rate Equations, Activation Energies, and Mechanisms. The experimental rate equation for reaction 1

$$UO_2^{2+}(aq) + HF(aq) \rightleftharpoons UO_2F^{+}(aq) + H^{+}(aq) \qquad (1)$$

is consistent with other mechanisms, in addition to the associative one discussed in the previous section (cf. ref 1). The present study gives strong support for a complex mechanism where the rate-determining step is the transfer of HF from the second to the first coordination sphere, without complete bond breaking in HF. The reaction is associative, with six-coordination in the transition state and a short U- - -FH distance of 2.6−2.7 Å. The strong reverse isotope effect observed in the exchange reaction 1 is in excellent agreement with the theory-based deductions; it is a ground-state effect due to the strong hydrogen bonding in the precursor and a small bond breaking in the entering HF in the rate determining step. The activation energy $\Delta U^{\neq} = 34$ kJ/mol is in good agreement with the experimental activation enthalpy $\Delta H^{\neq} = 38$ kJ/mol. An associative/interchange activation has been found also for the water exchange between $UO_2(H_2O)_5^{2+}$ and the bulk solvent, while exchange reactions for $UO_2F_5^{3-}$ and $UO_2F_4(H_2O)^{2-}$ are dissociative.

Acknowledgment. This work was supported by the Swedish National Allocation Committee (SNAC) via the allocation of the computer time at the National Supercomputer Center (NSC), Linköping, Sweden and by the Carl Trygger Foundation by a grant used to procure workstations. We wish to thank Dr. V. Vallet for fruitful discussions.

Supporting Information Available: Tables S1−S3, show the *xyz*- coordinates and the SCF gas-phase energies of the precursor and successor complexes discussed in the text in the order of appearance. Table S4 gives the thermal functions for precursor/successor complexes and Table S5 the corresponding thermal functions for Gibbs free energy and enthalpy of reaction. The material is available free of charge via the Internet at http://pubs.acs.org.

References and Notes

(1) (a) Szabó, Z.; Grenthe, I. *Inorg. Chem.* **1998**, *37*, 6214. (b) Morel, F. M. M.; Hering, J. G. *Principles and Applications of Aquatic Chemistry*, John Wiley and Sons: New York, 1983, p 399.

(2) Aas, W.; Szabó, Z.; Grenthe, I. *Dalton* **1999**, 1311.

(3) Farkas, I.; Bányai, I.; Szabó, Z.; Wahlgren, U.; Grenthe, I. *Inorg. Chem.* **2000**, *39*, 799.

(4) Vallet, V.; Wahlgren, U.; Schimmelpfennig, B.; Szabó, Z.; Grenthe, I. *J. Am. Chem. Soc.* **2001**, *123*, 11999.

(5) Vallet, V.; Wahlgren, U.; Szabó, Z.; Grenthe, I. *Inorg. Chem.* **2002**, *41*, 5626.

(6) Vallet, V.; Wahlgren, U.; Schimmelpfennig, B.; Moll, H.; Szabó, Z.; Grenthe, I. *Inorg. Chem.* **2001**, *40*, 3516.

(7) Szabó, Z.; Glaser, J.; Grenthe, I. *Inorg. Chem.* **1996**, *35*, 2036.

(8) Kuchle, W.; Dolg, M.; Stoll, H.; Preuss H. J. *J. Chem. Phys.* **1994**, *100*, 7535.

(9) Vallet, V.; Maron, L.; Schimmelpfennig, B.; Leininger, T.; Teichteil, C.; Gropen, O.; Grenthe, I.; Walhgren, U. *J. Phys. Chem. A* **1999**, *103*, 9285.

(10) Vallet, V.; Schimmelpfennig, B.; Maron, L.; Teichteil, C.; Leininger, T.; Gropen, O.; Grenthe, I.; Wahlgren, U. *Chem. Phys.* **1999**, *244*, 185.

(11) Maron, L.; Leininger, T.; Schimmelpfennig, B.; Vallet, V.; Heully, J.-L.; Teichteil, C.; Gropen, O.; Wahlgren, U. *Chem. Phys.* **1999**, *244*, 195.

(12) Küchle W, Diplomarbeit, **1993**.

(13) Bergner, A.; Dolg, M.; Küchle, W.; Stoll, H.; Preuss, H. J. *J. Mol. Phys.* **1993**, *80*, 1431.

(14) Huzinaga, S. *J. Chem. Phys.* **1965**, *42*, 1293.

(15) Anderson, K.; Barysz, M.; Bernhardsson, A.; Blomberg, M. R. A.; Carissan, Y.; Cooper, D. L.; Cossi, M.; Fleig, T.; Fulscher, M. P.; Gagliardi, L.; de Graaf, C.; Hess, B. A.; Karlstrom, G.; Lindh, R.; Malmqvist, P.-A.; Nakajima, T.; Neogrady, P.; Olsen, J.; Roos, B. O.; Schimmelpfennig, B.; Schutz, M.; Seijo, L.; Serrano-Andres, L.; Siegbahn, P. E. M.; Stalring, J.; Thorsteinsson, T.; Veryazov, V.; Widmark, P.-O. *MOLCAS*, version 5; Lund University: Sweden, 2002.

(16) Frisch, M. J.; Trucks, G. W.; Schlegel, H. B.; Scuseria, G. E.; Robb, M. A.; Cheeseman, J. R.; Zakrzewski, V. G.; Montgomery, J. A., Jr.; Stratmann, R. E.; Burant, J. C.; Dapprich, S.; Millam, J. M.; Daniels, A. D.; Kudin, K. N.; Strain, M. C.; Farkas, O.; Tomasi, J.; Barone, V.; Cossi, M.; Cammi, R.; Mennucci, B.; Pomelli, C.; Adamo, C.; Clifford, S.; Ochterski, J.; Petersson, G. A.; Ayala, P. Y.; Cui, Q.; Morokuma, K.; Malick, D. K.; Rabuck, A. D.; Raghavachari, K.; Foresman, J. B.; Cioslowski, J.; Ortiz, J. V.; Stefanov, B. B.; Liu, G.; Liashenko, A.; Piskorz, P.; Komaromi, I.; Gomperts, R.; Martin, R. L.; Fox, D. J.; Keith, T.; Al-Laham, M. A.; Peng, C. Y.; Nanayakkara, A.; Gonzalez, C.; Challacombe, M.; Gill, P. M. W.; Johnson, B. G.; Chen, W.; Wong, M. W.; Andres, J. L.; Head-Gordon, M.; Replogle, E. S.; Pople, J. A. *Gaussian 98*, revision A.9; Gaussian, Inc.: Pittsburgh, PA, 1998.

(17) Cossi, M.; Scalmani, G.; Rega, N.; Barone, V. *J. Phys. Chem. A.* **2002**, *117*, 43.

(18) Cossi, M.; Rega, N.; Scalmani, G.; Rega, N.; Barone, V. *J. Phys. Chem. A.* **2001**, *114*, 5691.

(19) Privalov, T.; Schimmelpfennig, B.; Wahlgren, U.; Grenthe, I. *J. Phys. Chem. A.* **2002**, *106*, 11277.

(20) Grenthe, I.; Fuger, J.; Konings, R. J. M.; Lemire, R. J.; Muller, A. B.; Nguyen-Trung, C.; Wanner, H. *Chemical Thermodynamics of Uranium*, North-Holland, 1992.

(21) Vallet, V.; Moll, H.; Wahlgren, U.; Szabó, Z.; Grenthe, I. *Inorg. Chem.* **2003**, *42*, 1982.